

# Calculation of the Field Distribution in a Railway Tunnel in Presence of Train Using Integrative Modelling Technique

#Shi Pu <sup>1,2</sup>, Jun-Hong Wang <sup>1,2</sup>, Yu-Jian Li <sup>1,2</sup>

<sup>1</sup>Institute of Lightwave Technology, Beijing Jiaotong University, Beijing 100044, China

<sup>2</sup>Key Laboratory of All Optical Network & Advanced Telecommunication Network, Education Ministry of China, Beijing Jiaotong University, Beijing 100044, China

#06111002@bjtu.edu.cn

## 1. Introduction

Within confined or semi-confined areas, the influence of environment on the propagation of radio waves is very significant, especially for the discrete antenna system. Commonly, radio wave coverage inside the tunnel for train-to-wayside communication is achieved using leaky coaxial cable (LCX), so it is important to know the property of the wireless radio wave link involving the LCX. Therefore, it is necessary to develop efficient method that can be used to model the whole wireless radio link based on LCX accurately. This is the motivation of this paper. The method in this paper can be divided into three parts (take downlink as example) [1, 2]: The radiating of radio frequency (RF) signal by LCX, the propagating of the wave in tunnel in presence of train, and the receiving of the RF signal by train antennas.

In fact, many efforts have been made in studying the tunnel and indoor propagation relative issues. However, the majority of these works are focused on the second part of the RF link as mentioned above, without considering the transmitting/receiving (Tx/Rx) components [3], or just simply considering the wave propagation as that in a relatively large hollow waveguide [4]. Regarding the LCX, some works about radio coverage prediction of radiating-mode LCX have been reported [5, 6]. These works could be applied to the cases of relatively empty tunnel or indoor scenarios, where the radiating wave of LCX can be treated as plane waves, so that the ray-tracing method can be used. However, for the complicated environment such as tunnel in presence of train, the ray-tracing based solutions are not accurate enough. In this paper, the FDTD method is employed to take into account not only the multi-path reflecting, scattering, diffracting, etc., but also the effects of Tx/Rx antennas.

## 2. Theory and Method

In this paper, definition of downlink of the RF wireless communication is starting from the LCX to the output terminal of the Rx antenna on train, while the uplink is starting from the input terminal of the Tx antenna on train to the LCX. Both links are used in the train-to-wayside communication system in railway tunnel, as shown schematically in Fig. 1. The system includes the LCX in tunnel, one base station (BS) at the entrance, and the other BS at the exit of the tunnel. The express train is running towards  $-y$ -direction with velocity of  $v$  and communicating with LCX installed in the rectangular railway tunnel. Four Tx/Rx antennas are mounted upon the train locomotive (called locomotive antennas) for different applications, and they are working at frequency of 900 MHz.

The FDTD method with Yee's mesh grid combined with the uni-axial anisotropic PML technique [1] are applied to model the whole system, including the LCX, locomotive antennas, and the surrounding environment. This scheme of modelling is called as the Integrative Modelling Technique (IMT).

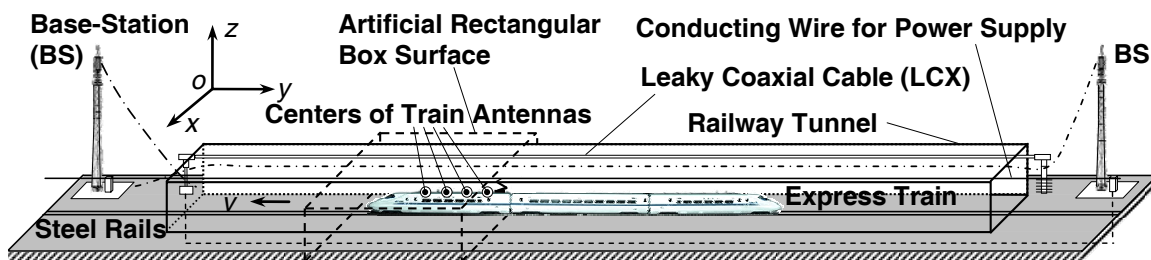


Figure 1: Schematic diagram of RF wireless link for train-to-wayside communication

Due to the limitations of computer memory and running time, the artificial rectangular closed surface which encloses the entire RF wireless link in the railway tunnel, as shown in Fig. 1, is restricted to the PML inner surface in the FDTD computation domain, as illustrated in Fig. 2. So only the significant environment is considered, which includes the locomotive of the train, tunnel walls, conducting wire for power supply, pantograph, steel rails and ballastless track. In FDTD, they are discretized into cubic meshes with grid size of  $\Delta S = 0.028$  m. The real target model and the uniformly meshed model of the train locomotive are depicted in Fig. 3. The locomotive has the maximum size of  $3.53 \text{ m} \times 24.83 \text{ m} \times 4.39 \text{ m}$  ( $127\Delta S \times 894\Delta S \times 158\Delta S$  correspondingly), and is located in the middle of the straight rectangular single track railway tunnel with width of  $5.5 \text{ m}$  and height of  $5.64 \text{ m}$ . The conducting wire for power supply has the cross-section size of  $1\Delta S \times 1\Delta S$  and is located  $0.72 \text{ m}$  ( $26\Delta S$ ) above the center of the locomotive top. Below the conducting wire, the  $1.56 \text{ m}$  long pantograph also with the cross-section size of  $1\Delta S \times 1\Delta S$  is placed. The other sizes and parameters are given in Fig. 2. The electromagnetic material parameters of the objects are listed in Table 1, where  $\mu_r$ ,  $\epsilon_r$  and  $\sigma$  denote the relative permeability, relative permittivity and electric conductivity respectively.

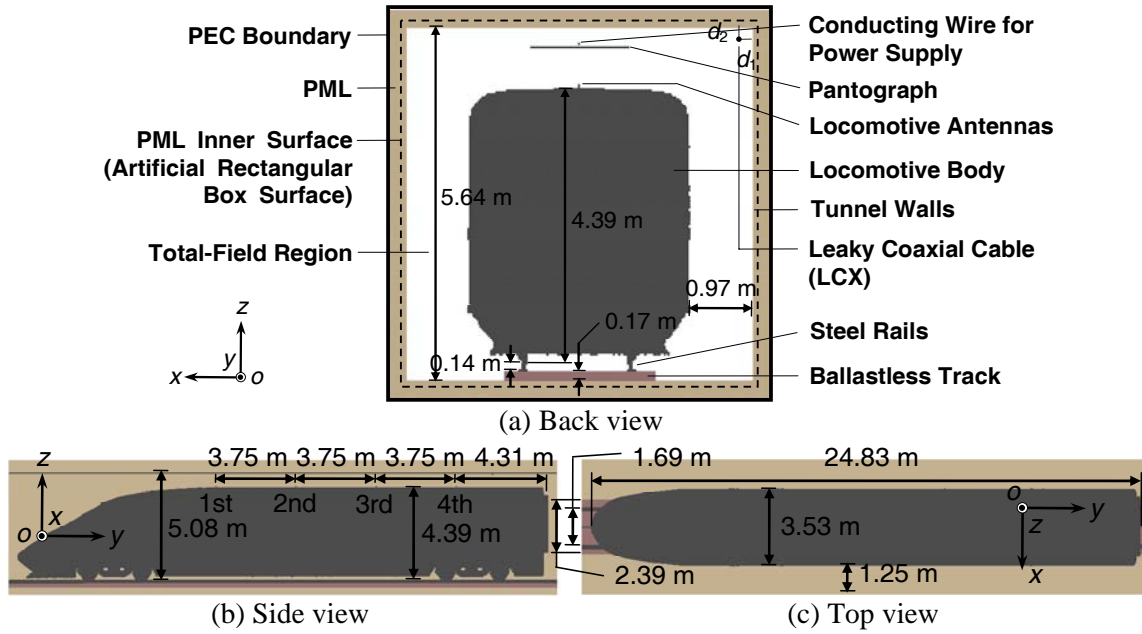


Figure 2: Cross-sections of FDTD computation domain for modelling entire RF wireless link

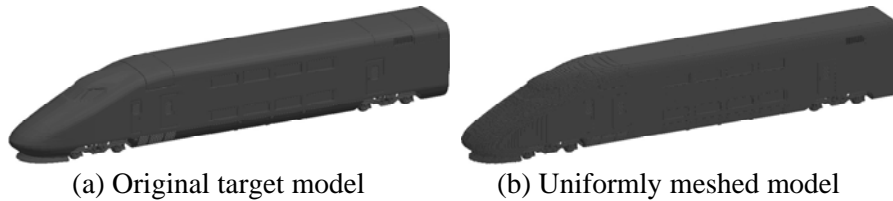


Figure 3: Three-dimensional geometric model of train locomotive body

Table 1: List of Electromagnetic Material Parameters Used

Object Model	$\mu_r$	$\epsilon_r$	$\sigma$ (S/m)	Object Model	$\mu_r$	$\epsilon_r$	$\sigma$ (S/m)
Locomotive Body	1.0	1.0	$2.494e+7$	Pantograph	1.0	1.0	$2.5e+5$
Tunnel Walls	1.0	6.8	$3.4e-2$	Steel Rails	1.0	1.0	$1.1e+6$
Conducting Wire for Power Supply	1.0	1.0	$5.8e+7$	Ballastless Track	1.0	6.0	$1.95e-3$

In this paper, the operating frequency for the whole system is set to  $900 \text{ MHz}$ . There are totally four quarter-wavelength monopole antennas mounted upon the locomotive along the central line. The antenna model used here is composed of the monopole arm part and coaxial line feeding part; they are simulated by thin-wire approximation and TEM-mode of coaxial cable respectively, as done in [2]. A radiating-mode LCX with inclined slot is used, as shown in Fig. 4, and there are two dual inclined slots carved in each period. According to the theory of LCX [7], this kind of structure could suppress

the  $-3$ th odd spatial harmonics and all the even spatial harmonics, and extend the single-mode band. As depicted in Fig. 4, the radiating LCX is approximated by an array of magnetic dipoles  $\mathbf{M}_l$ . In this paper, only the components in  $y$ -direction  $M_y$  are considered, since the Rx antennas are vertically mounted, and the vertical field component is mainly generated by  $M_y$ . In FDTD computation,  $M_y$  is introduced into the iterative formula of magnetic field  $H_y$ ,

$$H_y^{n+1/2}(i_s+1/2, j_s, k_s+1/2) = H_y^{n+1/2}(i_s+1/2, j_s, k_s+1/2) - \Delta t/(\mu_0 \Delta x \Delta y \Delta z) [M_y'(t)]^n \quad (1)$$

where  $H_y^{n+1/2}(i_s+1/2, j_s, k_s+1/2)$  represents the discretized magnetic field component used in FDTD,  $\Delta t$  is the time step,  $\mu_0$  denotes the permeability of free space, the grid size  $\Delta x = \Delta y = \Delta z = \Delta S$ , and  $M_y'(t)$  is the first order derivative of  $M_y(t)$  with respect to  $t$ . Here, the magnetic dipole source is set as

$$M_y(t) = M_0^l \cdot \sin[2\pi f_0 t - \beta_0 \varepsilon_{re}^{1/2} (d_s^l + (j_0 - 1)P)], l = 1, \dots, 4 \quad (2)$$

where  $l$  is the slot number in each period,  $P$  is the slot period, and  $M_0^l = -1$  for  $l = 1$  or  $2$ ,  $M_0^l = +1$  for  $l = 3$  or  $4$ .  $\beta_0$  is the wavenumber in free space,  $\varepsilon_{re}$  is the relative permittivity of the coaxial dielectric,  $d_s^l$  is the distance between the slot  $l$  and the first slot ( $l = 1$ ) in each period, and  $j_0$  represents the  $j_0$ th period. Through this method, the LCX is integrated into the FDTD computation.

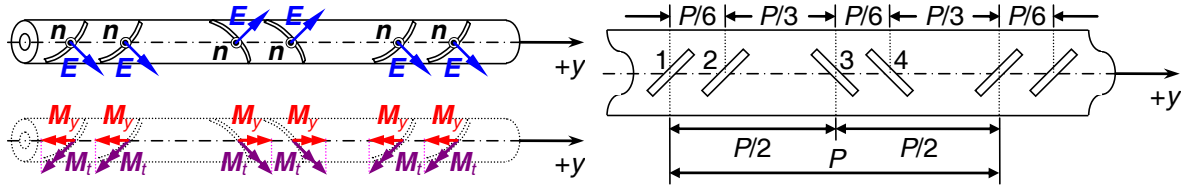


Figure 4: Example of a radiating-mode inclined slot LCX and its equivalent approximation

### 3. Numerical Results and Discussion

The integrative modelling technique presented above was applied to calculate the field distributions under the railway tunnel communication environment. As shown in Fig. 2, the whole FDTD computation domain is divided into  $218 \times 924 \times 223$  cells, including the outer 8 cells for PML. The space step and time step are set to  $\Delta S = 0.028$  m and  $\Delta t = \Delta S/(2c) = 0.046$  ns respectively, where  $c$  is the velocity of light. The four locomotive antennas and their feeding coaxial cables have the same parameters: the radius of inner conductor is  $a = 2.53$  mm, the radius of inner surface of outer conductor is  $b = 5.82$  mm, and the coaxial dielectric is  $\varepsilon_r = 1.0$ . Here, the 1st, 3rd and 4th locomotive antennas are taken as the Tx antennas, while the 2nd locomotive antenna is treated as the Rx antenna. By exciting the three Tx antennas separately, the field distributions in the rectangular railway tunnel in  $zox$ -plane are obtained and the amplitude distributions of  $E_z$  given in Fig. 5. In this situation, the amplitude of the voltage source applied to the locomotive antenna is set to 1 V. From this figure, it is seen that the field strength level in the area beyond locomotive top is much higher than that in other areas. Thereby, the LCX should be laid at suitable position to acquire reliable signal. Usually, the LCX is hung on one side of the tunnel walls with distances  $d_1$  and  $d_2$  to the side and top, as shown in Fig. 2. By exciting the LCX at  $d_1 = 0.19$  m, and  $d_2 = 0.19$  m,  $0.47$  m,  $0.75$  m and  $1$  m respectively, the field distributions of  $|E_z|$  in the tunnel in  $xoy$ -plane through the locomotive top surface and the feeding points of locomotive antennas are obtained and given in Fig. 6. The parameters of the LCX used here are  $\varepsilon_{re} = 1.18$  and  $P = 33.4$  cm, so it is working in the mono-harmonic radiating-mode. The included angle between the radiation direction of  $-1$ th spatial harmonics and  $+y$ -direction is given by  $\theta_{-1} = \cos^{-1}[\varepsilon_{re}^{1/2} - c/(f_0 P)] = 85^\circ$ , which is also indicated by the yellow areas in the left of Fig. 6. It is found that the influence of the locomotive body and tunnel environment on the field distribution is very significant, and the field coverage on the locomotive top where the antennas mounted, seems more homogenous when the LCX is installed higher.

### 4. Conclusions

Estimation of the radio coverage inside a railway tunnel is a very important work. To include the Tx/Rx antennas and the effect of the environment, an integrative modeling technique involving the FDTD method and PML technique is applied to simulate the entire RF wireless link, which is starting from the input of the LCX to the output of the locomotive antennas via the tunnel space (downward). The LCX and locomotive antennas are modelled as an array of magnetic dipoles and four coax-fed quarter-wavelength monopoles respectively. The field distributions in a straight rectangular shaped

single track railway tunnel are calculated under the excitations of the LCX and locomotive antennas separately. From the results, we can conclude that the interactions between Tx/Rx antennas and environment could not be neglected in such confined areas, and smoother field coverage would be obtained if the LCX is laid higher on side tunnel wall.

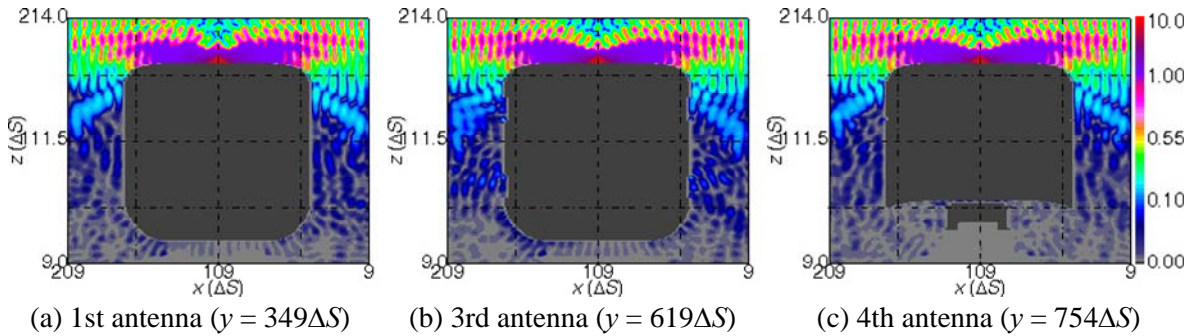


Figure 5: Field distributions in railway tunnel under excitations of locomotive antenna

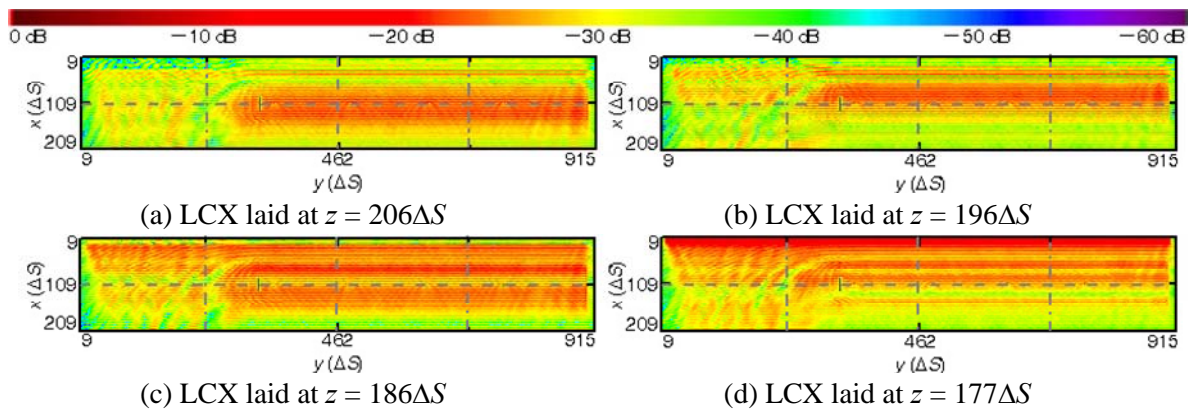


Figure 6: Field distributions in railway tunnel under excitations of LCX at different positions

## Acknowledgments

This work was supported by NSFC under grant no. 60825101, National High-Tech R&D Program of China (863) under grant 2008AA01Z224, and the PCSIRT, MOE, China under grant no. IRT0707.

## References

- [1] S. Pu, J.-H. Wang, "Research on the receiving and radiating characteristics of antennas on high-speed train using integrative modeling technique," Proc. 11th Asia Pacific Microwave Conference, Singapore, pp. 1072-1075, 2009.
- [2] S. Pu, J.-H. Wang, Z. Zhang, "Estimation for small-scale fading characteristics of RF wireless link under railway communication environment using integrative modeling technique," Progress In Electromagnetics Research-PIER, Vol. 106, pp. 395-417, 2010.
- [3] Y. P. Zhang, Y. Hwang, "Theory of the radio-wave propagation in railway tunnels," IEEE Transactions on Vehicular Technology, Vol. 47, No. 3, pp. 1027-1036, 1998.
- [4] A. M. Ghuniem, "Modes of electromagnetic wave propagation in circular concrete tunnels," Journal of Electromagnetic Waves and Applications, Vol. 19, No. 1, pp. 95-106, 2005.
- [5] S. P. Morgan, "Prediction of indoor wireless coverage by leaky coaxial cable using ray tracing," IEEE Transactions on Vehicular Technology, Vol. 48, No. 6, pp. 2005-2014, 1999.
- [6] H. Cao, Y. P. Zhang, "Radio propagation along a radiated mode leaky coaxial cable in tunnels," Proc. 4th Asia Pacific Microwave Conference, Singapore, pp. 270-272, 1999.
- [7] J. H. Wang, K. K. Mei, "Design and calculation of the directional leaky coaxial cables," Radio Science, Vol. 36, No. 4, pp. 551-558, 2001.